Nanoscale

CrossMark
click for updates

Valence holes observed in nanodiamonds dispersed in water†

Tristan Petit,*‡[a] Mika Pflüger,‡[b] Daniel Tolksdorf,[b] Jie Xiao[a] and Emad F. Aziz[a,b,c]

Colloidal dispersion is essential for most nanodiamond applications, but its influence on nanodiamond electronic properties remains unknown. Here we have probed the electronic structure of oxidized detonation nanodiamonds dispersed in water by using soft X-ray absorption and emission spectroscopies at the carbon and oxygen K edges. Upon dispersion in water, the π^* transitions from sp^2-hybridized carbon disappear, and holes in the valence band are observed.

Understanding the impact of water colloidal dispersion on the electronic properties of nanodiamonds (NDs) is critical as many of their applications, such as biomedical imaging and drug delivery, take place in an aqueous environment.[1] Electronic interactions with water or other neighboring molecules in an aqueous environment are believed to influence their colloidal,[2–5] luminescence[6,7] and catalytic[8,9] properties. For drug delivery applications, it was observed that the addition of salt[10,11] or change of pH[12] has an impact on the drug absorption, which may also be related to the changes in the electronic structure of ND surface states. However, only basic electrostatic information, such as the Zeta potential measured by electrophoretic light scattering, are currently available to monitor *in situ* changes in the electronic structure of NDs in water. Detailed information about occupied and unoccupied electronic states in the valence and conduction bands, respectively, for NDs in solution is still missing. Electronic interactions between the NDs and the surrounding molecules, including bond-building/breaking and charge transfer, would strongly affect these electronic states.

Core-level spectroscopy at the K-edge of oxygen and carbon is a powerful method to characterize the electronic properties of NDs in water because it is element-specific and can provide information on the electronic and chemical states of the investigated systems.[13,14] X-ray absorption (XA) and X-ray emission (XE) spectroscopies are complementary methods probing the unoccupied and occupied electronic density of states of the probed materials, respectively. Characterization of NDs in aqueous media with XAS and XES remains particularly challenging as vacuum conditions are necessary to take into account the short penetration depth of soft X-ray photons required to probe the K edges of carbon and oxygen atoms. Consequently, NDs are usually dried on a substrate or a grid before analysis under vacuum. However, it remains questionable whether the electronic structure measured under such conditions can be extrapolated to an aqueous environment. For example, electronic interaction with an underlying substrate cannot be ruled out,[15] and charge transfers to solvent or other dissolved molecules are dynamic processes,[16] which cannot be easily reproduced *ex situ*.

The microjet technique, which allows measurement of liquids under vacuum conditions by soft X-ray spectroscopies, was introduced in the 90s.[17] Combined with the high brilliance of current synchrotron facilities, this technique is particularly efficient to characterize dissolved ions and small molecules in various solvents.[14] Although, first studies of XAS were recently reported with dispersed cobalt,[18] silica[19] and ceria[20] nanoparticles, characterization of nanomaterials in suspension remains scarce. XAS and XES are based on photon-in/photon-out processes and are therefore sensitive to nanoparticles in the bulk of the microjet, complementary to the X-ray photoelectron spectroscopy (XPS) which has been applied to probe surface layers of nanoparticles in water due to the very short mean free path of electrons.[21]

In this study, carbon and oxygen K edges of oxidized detonation NDs dispersed in water at 1 wt% were characterized by synchrotron-based XAS measured in total fluorescence yield (TFY) mode and XES. NDs in aqueous solution, probed using a liquid microjet (ND-mj), were compared to a thin compact layer of NDs dried on a silicon substrate (ND-sub), to observe the effect of water dispersion.

XAS and XES measurements at the carbon K edge of ND-sub and ND-mj are compared in Fig. 1. The XE spectra,

[a]*Institute of Methods for Materials Development, Helmholtz-Zentrum Berlin, Albert-Einstein-Str. 15, 12489 Berlin, Germany. E-mail: tristan.petit@helmholtz-berlin.de*
[b]*Freie Universität Berlin, FB Physik, Arnimallee 14, 14195 Berlin, Germany*
[c]*Institute of Molecular Science, Myodaiji, Okazaki, 444-8585, Japan*

‡These authors contributed equally to the work.
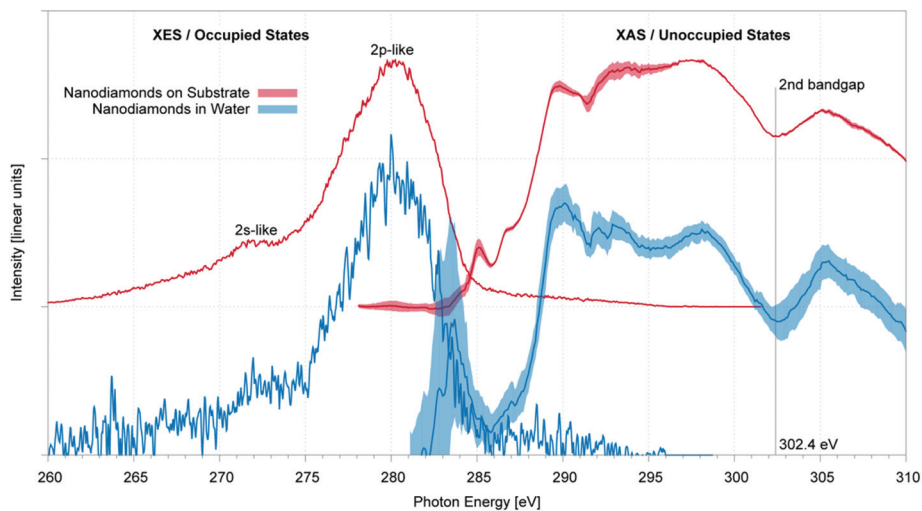
Fig. 1 Carbon K edge XES (left) and XAS (right) measurements of ND–sub (red) deposited on a silicon substrate and ND–mj (blue) dispersed in water at 1 wt%. The standard deviation is indicated by lighter color for XAS measurements.

obtained by non-resonant excitation at 320 eV, are constituted of a broad peak at 280.0 eV and a smaller feature at 272.0 eV for both liquid and solid samples, attributed to occupied electronic states with 2p and 2s character, respectively.[22] These features, corresponding to the valence band of NDs, are comparable to previous XES reports on ND thin films[23,24] and no significant differences are observed between ND-sub and ND-mj except for a higher noise level of ND-mj.

The resonant excitations at the carbon K edge were also conducted but no excitation energy-dependent features were observed for excitation energies above the edge. This is different from a bulk single-crystal diamond that clearly shows peak shifts as the excitation energy varies associated with resonant inelastic X-ray scattering (RIXS).[25] The imperfect crystalline structure of detonation NDs[26] leads to incoherent scattering, which is not excitation energy dependent.[25] Therefore the off-resonant XES features representing the occupied states are expected even when the system is excited resonantly.

For XA spectra at the carbon K edge, a dip at 302.4 eV related to the second absolute band gap of a diamond and a band at 293 eV related to C 1s to σ* transitions for sp³-hybridized carbon atoms are clearly visible for both samples. These features demonstrate that the electronic structure of the diamond core of the NDs remains unchanged with water dispersion. The excitonic peak at 289.6 eV appears up-shifted and broadened compared to a bulk diamond, which was previously attributed to quantum confinement.[27,28] The features in the energy range of 295–310 eV are slightly more pronounced for ND-mj than for ND-sub. One of the possible reasons could be that the saturation effect related to TFY measurement[29] is reduced for ND-mj due to its lower carbon concentration. Indeed, ND-sub is constituted of a compact layer of NDs lying on a substrate so that the incident X-rays are fully absorbed by the NDs and therefore the TFY–XA spectrum appears saturated. In contrast, NDs dispersed at low concentration in water

absorbs only a fraction of the incident beam; hence ND-mj are less sensitive to saturation.

A detailed analysis of the pre-edge region of the XA spectrum, shown in Fig. 2, provides information on the chemical bonding and the electronic state of the ND surface. The XE spectrum of ND-sub is also presented in Fig. 2 to indicate the energy range of the occupied states. A feature is observed at 286.7 eV on both samples, which can be attributed either to fullerene-like reconstructions (FLRs)[23] or to C=O bonds.[30,31] FLRs are likely to be present on detonation NDs, while C=O
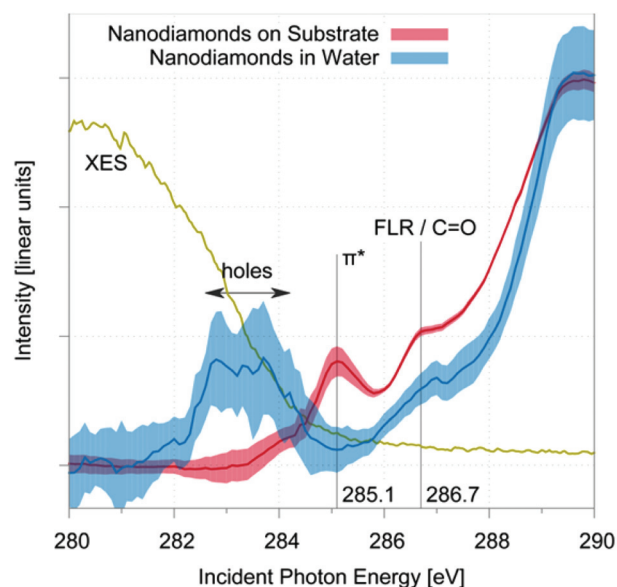
Fig. 2 XAS pre-edge region of ND-sub (red) and ND-mj (blue) dispersed in water at 1 wt%. The ND-mj XA spectrum is an average of 7 independent measurements. The standard deviation is indicated by lighter color. XES from ND-sub (green) is also plotted to indicate the energy range of occupied states in the NDs valence band.

bonds from carboxyl or carbonyl groups are expected for oxidized NDs. Another peak is detected at 285.1 eV on ND-sub, associated with π* transitions from sp²-hybridized carbon atoms as reported previously.[23,27,30] Interestingly, no peak appears at this energy on ND-mj.

Another difference between ND-sub and ND-mj is the appearance of a broad band around 283 eV, only observed on ND-mj. This feature lies in the valence band of NDs, as indicated by the XE spectrum (Fig. 2). Although, a significant photon flux loss from the beamline is observed in this energy range, the peak is clearly resolved after a careful correction for photon flux and background signal (see ESI†). In the following, we discuss the observation of valence band holes in our study in the light of earlier literature reports.[4,5,16,32–35]

Previously, empty states in the valence band were already observed by XAS on a bulk diamond when highly doped by boron atoms.[32,33] As reported by Zegkinoglou et al., two peaks are measured at 284.0 and 282.5 eV attributed to boron acceptors in the diamond matrix and to transitions from this boron acceptor to adjacent carbon atoms, respectively.[33] Although, small boron contamination due to the surface purification process have been reported on NDs used in this study,[36] substitution in the diamond matrix is necessary to induce a hole signature for the XA spectrum at the carbon K edge. In the case of accidental boron incorporation in the diamond matrix of NDs, holes induced by boron impurities should also be visible on ND-sub, therefore this origin can be ruled out.

Other studies on the undoped bulk diamond have also reported a feature at 282.5 eV when the diamond surface is unsaturated, for example, after in situ high temperature annealing under UHV[34,37] or partial hydrogen plasma treatment.[35] These unoccupied states were attributed to π-bonded single dangling bonds on clean diamond C(100) − (2 × 1) surface resulting from a partial hydrogenation.[35] This interpretation cannot fit to our case because these dangling bonds are only stable under ultrahigh vacuum and would certainly be rapidly saturated in water.

Another origin for valence holes could be related to surface band bending induced by charge transfer in an aqueous environment. Charge transfer involving electrochemical redox couples in water was already reported on the hydrogenated bulk diamond[16] and NDs.[5] However, NDs used in our study were not hydrogenated and oxygen termination should prevent charge transfer.[16] Nevertheless, the surface chemistry of detonation NDs is diverse and other surface structures, such as FLRs,[4] may also be sensitive to electronic interactions in aqueous solutions. Indeed, graphene layers were also previously found to be sensitive to p-doping induced by similar charge transfer in the presence of oxygen and water molecules.[38,39] Furthermore, spontaneous polarization at the diamond–FLRs interface induce migration of free electrons to the graphene surface layer,[11] which is then more sensitive to hole doping. From our XAS results, we have a clear signature of holes in the valence band of NDs. Water solvation plays a crucial role in the hole formation because they are not detected on XAS from dried NDs. Hole doping induced by elec-

tron transfer involving a O_2/H_2O redox couple on FLRs seems therefore to be the most likely explanation for the origin of these holes.

The disappearance of π* transitions on NDs after water dispersion is consistent with hole doping on FLRs. Indeed, the sp² signature of surface-graphitized NDs was previously found to vanish after air exposure and water dispersion based on XPS measurements under vacuum.[4] The disappearance was attributed to chemisorption of molecular oxygen on graphitic planes. A similar surface evolution was reported by Shpilman et al. on a reconstructed single-crystal diamond surface characterized by XAS.[30] After in situ exposure to molecular oxygen under ultrahigh vacuum, the intensity of the peak related to amorphous sp² and defect states at 283.9 eV is strongly reduced while new components appear at 282.65 and 286.6 eV. In water, the electronic interaction between molecular oxygen and the ND surface is probably different from ultrahigh vacuum. Nevertheless, adsorption of dissolved electron acceptors, such as molecular oxygen, on FLRs is apparently stabilized by water dispersion, which could be an explanation for the disappearance of π* transitions on ND-mj. Although, the exact charge transfer mechanism remains to be determined, our experimental results strongly support the idea of electron transfer from NDs to molecules, probably molecular oxygen, adsorbed on FLRs.

At first sight, observing holes in the valence band of NDs studied here seems to contradict with the negative Zeta potential induced by carboxylate groups on their surface. Nevertheless, it is very likely that the positive charges from holes are screened by negative charges of carboxylate groups due to the stronger charge density of ionizable surface sites.[16] For NDs without ionizable surface functional groups such as carboxylate groups, holes would be the main surface charges and would turn the Zeta potential to positive values, as observed on hydroxylated,[40] hydrogenated[3,5] or surface-graphitized NDs.[4]

In order to see the effect of the NDs on the local electronic structure of water we have performed oxygen K edge XAS and XES on ND-mj as shown in Fig. 3. Non-resonant XES is known to be sensitive to the hydrogen bond network of water.[41,42] The intensity of the two components d_1 and d_2 of the splitting of the $1b_1$ orbital of water was previously used to characterize changes of the water hydrogen bond network induced by ions dissolved in water.[43,44]

With NDs, no clear changes are detected compared to pure water in Fig. 3a, suggesting that modification of the water structure is not sufficient to be detected by XES for NDs concentration of 1 wt%. For XAS measurement (Fig. 3b), the spectra are dominated by the water contribution, which is expected considering the low concentration of oxygen atoms coming from surface groups of NDs compared to water molecules. A shoulder at 531.4 eV is though detected below the pre-edge of water for NDs concentration of 5 wt%, corresponding to the O 1s to π* transitions of C=O bonds from NDs surface functional groups. Note that this component is downshifted compared to acetate molecules probed under similar conditions.[43]
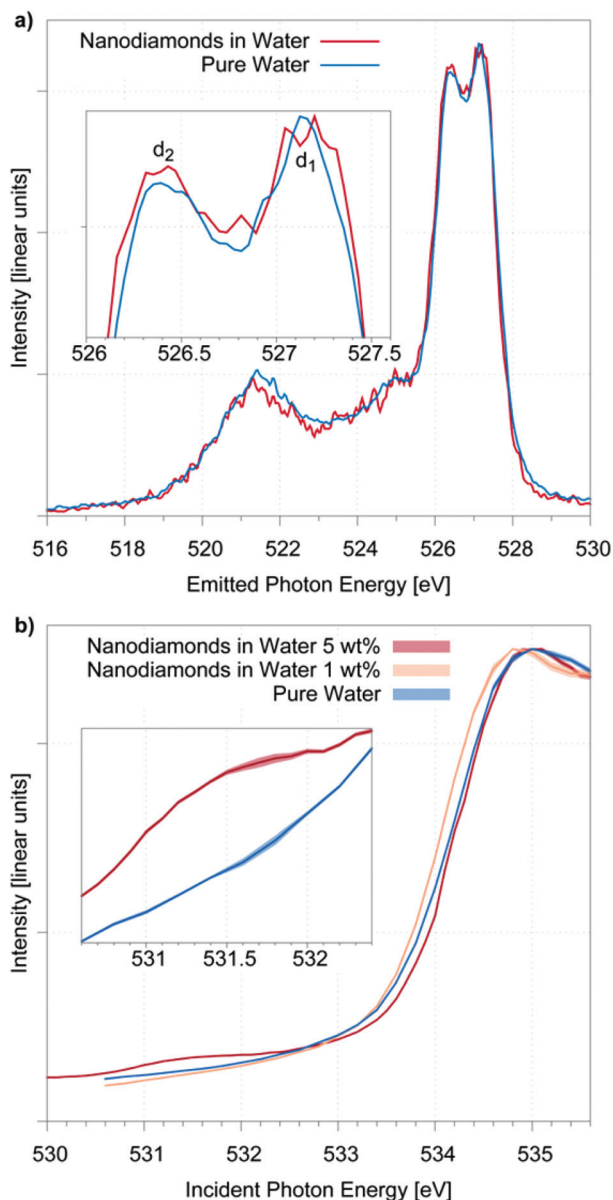
Fig. 3 (a) Non-resonant XES of oxygen K edge recorded at an excitation energy of 540 eV for pure water (blue) and ND-mj at 1 wt% (red). Inset shows a magnification of the splitting of the $1b_1$ orbital of water. (b) Oxygen K edge XAS measurements of pure water (blue) and ND-mj dispersed in water at 1 (orange) and 5 wt% (red). Spectra were calibrated and normalized to the water pre-edge feature at 535.0 eV. Magnification of π^* transitions of C=O bonds from ND-mj 5 wt% is plotted in the inset.

In summary, we have demonstrated in this study that the π^* transitions from sp²-hybridized surface states, present on dried NDs, disappear upon dispersing the NDs in water. On the other hand, valence holes are observed for NDs in water, which might be related to the electron transfer from the ND surface to the surrounding water molecules or other species present in aqueous solution. Such holes would probably affect the colloidal, optical, chemical and catalytic properties of NDs dispersed in water. Further studies are necessary to better understand their origin and structure. Similar electronic effects are likely to occur also on sp²-based nanocarbons in aqueous dispersions, and would be worth investigating.

Acknowledgements

Notes and references

1 V. N. Mochalin, O. Shenderova, D. Ho and Y. Gogotsi, *Nat. Nanotechnol.*, 2012, **7**, 11–23.
2 M. Ozawa, M. Inaguma, M. Takahashi, F. Kataoka, a. Krüger and E. Ōsawa, *Adv. Mater.*, 2007, **19**, 1201–1206.
3 O. A. Williams, J. Hees, C. Dieker, W. Jäger, L. Kirste, C. E. Nebel and W. Jäger, *ACS Nano*, 2010, **4**, 4824–4830.
4 T. Petit, J.-C. C. Arnault, H. A. Girard, M. Sennour, T.-Y. Kang, C.-L. Cheng and P. Bergonzo, *Nanoscale*, 2012, **4**, 6792–6799.
5 T. Petit, H. A. Girard, A. Trouvé, I. Batonneau-Gener, P. Bergonzo and J.-C. Arnault, *Nanoscale*, 2013, **5**, 8958–8962.
6 V. Petráková, A. Taylor, I. Kratochvílová, F. Fendrych, J. Vacík, J. Kučka, J. Štursa, P. Cígler, M. Ledvina, A. Fišerová, P. Kneppo and M. Nesládek, *Adv. Funct. Mater.*, 2012, **22**, 812–819.
7 T. A. Dolenko, S. A. Burikov, J. M. Rosenholm, O. A. Shenderova and I. I. Vlasov, *J. Phys. Chem. C*, 2012, **116**, 24314–24319.
8 D. M. Jang, Y. Myung, H. S. Im, Y. S. Seo, Y. J. Cho, C. W. Lee, J. Park, A.-Y. Jee and M. Lee, *Chem. Commun.*, 2012, **48**, 696–698.
9 D. Zhu, L. Zhang, R. E. Ruther and R. J. Hamers, *Nat. Mater.*, 2013, **12**, 836–841.
10 H. Huang, E. Pierstorff, E. Osawa and D. Ho, *Nano Lett.*, 2007, **7**, 3305–3314.
11 E. Ōsawa, D. Ho, H. Huang, M. V. Korobov and N. N. Rozhkova, *Diamond Relat. Mater.*, 2009, **18**, 904–909.
12 A. Adnan, R. Lam, H. Chen, J. Lee, D. J. Schaffer, A. S. Barnard, G. C. Schatz, D. Ho and W. K. Liu, *Mol. Pharm.*, 2011, **8**, 368–374.
13 F. de Groot and A. Kotani, *Core Level Spectroscopy of Solids*, Taylor & Francis, New York, 2008.
14 K. M. Lange and E. F. Aziz, *Chem. Soc. Rev.*, 2013, **42**, 6840–6859.
15 S. Stehlik, T. Petit, H. A. Girard, J.-C. Arnault, A. Kromka and B. Rezek, *Langmuir*, 2013, **29**, 1634–1641.
16 V. Chakrapani, J. C. Angus, A. B. Anderson, S. D. Wolter, B. R. Stoner and G. U. Sumanasekera, *Science*, 2007, **318**, 1424–1430.

17 M. Faubel, B. Steiner and J. P. Toennies, *J. Chem. Phys.*, 1997, **106**, 9013.

18 H. Liu, Y. Yin, A. Augustsson, C. Dong, J. Nordgren, C. Chang, P. Alivisatos, G. Thornton, D. F. Ogletree, F. G. Requejo, F. de Groot and M. Salmeron, *Nano Lett.*, 2007, **7**, 1919–1922.

19 M. A. Brown, T. Huthwelker, A. Beloqui Redondo, M. Janousch, M. Faubel, C. A. Arrell, M. Scarongella, M. Chergui and J. A. van Bokhoven, *J. Phys. Chem. Lett.*, 2012, **3**, 231–235.

20 J.-D. Cafun, K. O. Kvashnina, E. Casals, V. F. Puntes and P. Glatzel, *ACS Nano*, 2013, **7**, 10726–10732.

21 M. A. Brown, R. Seidel, S. Thürmer, M. Faubel, J. C. Hemminger, J. A. van Bokhoven, B. Winter and M. Sterrer, *Phys. Chem. Chem. Phys.*, 2011, **13**, 12720–12723.

22 K. Endo, S. Koizumi, T. Otsuka, T. Ida, T. Morohashi, J. Onoe, A. Nakao, E. Z. Kurmaev, A. Moewes and D. P. Chong, *J. Phys. Chem. A*, 2003, **107**, 9403–9408.

23 J.-Y. Raty, G. Galli, C. Bostedt, T. W. van Buuren and L. J. Terminello, *Phys. Rev. Lett.*, 2003, **90**, 37401.

24 T. Hamilton, E. Z. Kurmaev, S. N. Shamin, P. Y. Detkov, S. I. Chukhaeva and A. Moewes, *Diamond Relat. Mater.*, 2007, **16**, 350–352.

25 Y. Ma, N. Wassdahl, P. Skytt, J. Guo, J. Nordgren, P. Johnson, J.-E. Rubensson, T. Boske, W. Eberhardt and S. Kevan, *Phys. Rev. Lett.*, 1992, **69**, 2598–2601.

26 X. Fang, J. Mao, E. M. Levin and K. Schmidt-Rohr, *J. Am. Chem. Soc.*, 2009, **131**, 1426–1435.

27 Y. Chang, H. Hsieh, W. Pong, M.-H. Tsai, F. Chien, P. Tseng, L. Chen, T. Wang, K. Chen, D. Bhusari, J. Yang and S. Lin, *Phys. Rev. Lett.*, 1999, **82**, 5377–5380.

28 T. Berg, E. Marosits, J. Maul, P. Nagel, U. Ott, F. Schertz, S. Schuppler, C. Sudek and G. Schönhense, *J. Appl. Phys.*, 2008, **104**, 064303.

29 S. Eisebitt, T. Böske, J.-E. Rubensson and W. Eberhardt, *Phys. Rev. B: Condens. Matter*, 1993, **47**, 14103–14109.

30 Z. Shpilman, I. Gouzman, T. K. Minton, L. Shen, A. Stacey, J. Orwa, S. Prawer, B. C. C. Cowie and A. Hoffman, *Diamond Relat. Mater.*, 2014, **45**, 20–27.

31 A. Wolcott, T. Schiros, M. E. Trusheim, E. H. Chen, D. Nordlund, R. E. Diaz, O. Gaathon, D. Englund and J. S. Owen, *J. Phys. Chem. C*, 2014, **118**, 26695–26702.

32 J. Nakamura, E. Kabasawa, N. Yamada, Y. Einaga, D. Saito, H. Isshiki, S. Yugo and R. Perera, *Phys. Rev. B: Condens. Matter*, 2004, **70**, 245111.

33 I. Zegkinoglou, P. L. Cook, P. S. Johnson, W. Yang, J. Guo, D. Pickup, R. González-Moreno, C. Rogero, R. E. Ruther, M. L. Rigsby, J. E. Ortega, R. J. Hamers and F. J. Himpsel, *J. Phys. Chem. C*, 2012, **116**, 13877–13883.

34 A. Laikhtman and A. Hoffman, *Diamond Relat. Mater.*, 2002, **11**, 371–377.

35 K. Bobrov, G. Comtet, G. Dujardin, L. Hellner, P. Bergonzo and C. Mer, *Phys. Rev. B: Condens. Matter*, 2001, **63**, 165421.

36 D. P. Mitev, A. T. Townsend, B. Paull and P. N. Nesterenko, *J. Mater. Sci.*, 2014, **49**, 3573–3591.

37 J. Morar, F. Himpsel, G. Hollinger, J. Jordon, G. Hughes and F. McFeely, *Phys. Rev. B: Condens. Matter*, 1986, **33**, 1346–1349.

38 S. Ryu, L. Liu, S. Berciaud, Y.-J. Yu, H. Liu, P. Kim, G. W. Flynn and L. E. Brus, *Nano Lett.*, 2010, **10**, 4944–4951.

39 P. L. Levesque, S. S. Sabri, C. M. Aguirre, J. Guillemette, M. Siaj, P. Desjardins, T. Szkopek and R. Martel, *Nano Lett.*, 2011, **11**, 132–137.

40 O. Shenderova, A. M. Panich, S. Moseenkov, S. C. Hens, V. Kuznetsov and H. M. Vieth, *J. Phys. Chem. C*, 2011, **115**, 19005–19011.

41 K. M. Lange, R. Könnecke, M. Soldatov, R. Golnak, J.-E. Rubensson, A. Soldatov and E. F. Aziz, *Angew. Chem., Int. Ed.*, 2011, **50**, 10621–10625.

42 K. M. Lange, M. Soldatov, R. Golnak, M. Gotz, N. Engel, R. Könnecke, J.-E. Rubensson and E. F. Aziz, *Phys. Rev. B: Condens. Matter*, 2012, **85**, 155104.

43 T. Petit, K. M. Lange, G. Conrad, K. Yamamoto, C. Schwanke, K. F. Hodeck, M. Dantz, T. Brandenburg, E. Suljoti and E. F. Aziz, *Struct. Dyn.*, 2014, **1**, 034901.

44 R. Golnak, K. Atak, E. Suljoti, K. F. Hodeck, K. M. Lange, M. A. Soldatov, N. Engel and E. F. Aziz, *Phys. Chem. Chem. Phys.*, 2013, **15**, 8046–8049.